ORIGINAL RESEARCH

# Hemin Causes Lung Microvascular Endothelial Barrier Dysfunction by Necroptotic Cell Death

Sunit Singla, Justin R. Sysol, Benjamin Dille, Nicole Jones, Jiwang Chen, and Roberto F. Machado

Division of Pulmonary, Critical Care, Sleep, and Allergy Medicine, Department of Medicine, University of Illinois, Chicago, Illinois

## Abstract

Hemin, the oxidized prosthetic moiety of hemoglobin, has been implicated in the pathogenesis of acute chest syndrome in patients with sickle cell disease by virtue of its endothelial-activating properties. In this study, we examined whether hemin can cause lung microvascular endothelial barrier dysfunction. By assessing transendothelial resistance using electrical cell impedance sensing, and by directly measuring *trans*-monolayer fluorescein isothiocyanate-dextran flux, we found that hemin does cause endothelial barrier dysfunction in a concentration-dependent manner. Pretreatment with either a Toll-like receptor 4 inhibitor, TAK-242, or an antioxidant, N-acetylcysteine, abrogated this effect. Increased monolayer permeability was found to be associated with programmed cell death by necroptosis, as evidenced by Trypan blue staining, terminal deoxynucleotidyl transferase dUTP nick-end labeling assay, Western blotting for activated forms of key effectors of cell death pathways, and studies utilizing specific inhibitors of necroptosis and apoptosis. Further studies examining the role of endothelial cell necroptosis in promoting noncardiogenic pulmonary edema during acute chest syndrome are warranted and may open a new avenue of potential treatments for this devastating disease.

**Keywords:** hemin; sickle cell disease; acute chest syndrome; endothelial cell; necroptosis

### Clinical Relevance

This study describes for the first time the role of necroptotic cell death in the mechanisms of hemin-induced pulmonary vascular leak, which underlies acute chest syndrome. Further studies of the role of endothelial necroptosis in this disease process may open a new avenue for the development of acute chest syndrome therapies.

Acute chest syndrome (ACS) is a pulmonary complication of sickle cell disease (SCD) and is a leading cause of respiratory failure and mortality in patients with SCD (1). It consists of fever, cough, chest or bone pain, hypoxemia, and an associated new pulmonary infiltrate on radiography (2). The pathogenesis of ACS is not completely understood, but given its clinical association with vaso-occlusive pain crises in patients with SCD (3, 4), it is thought to involve pulmonary microvascular stasis and thrombosis by polymerized sickle erythrocytes. The role of vascular endothelial barrier dysfunction in ACS pathogenesis remains unclear but is posited to exist, since the spectrum of ACS severity includes cases of progression to diffuse noncardiogenic pulmonary edema (5), as occurs in acute respiratory distress syndrome (ARDS).

Recently, the oxidized prosthetic moiety of hemoglobin, hemin, has been implicated as a key danger-associated molecular-pattern molecule that is released during the intravascular hemolysis and enhanced auto-oxidation that usually precedes the onset of ACS in patients with SCD (6–8). Hemin has been shown to activate vascular endothelial cells (ECs) via Toll-like receptor 4 (TLR4) and reactive oxygen species (ROS) signaling, leading to Weibel-Palade body degranulation, NF-κB activation, leukocyte adhesion, and microvascular vaso-occlusion in sickle mice (9). Additionally, Ghosh and colleagues established the only known preclinical model for ACS by infusing low-dose hemin in transgenic sickle mice (6). TLR4 and downstream ROS signaling are key mediators of hemin-induced ACS in this model.

(Received in original form September 6, 2016; accepted in final form April 8, 2017)

The work was supported by National Institutes of Health grants 1R01HL133951–01, 1R01HL127342–01A1, and 4R01HL111656–04 (R.F.M.).

Author Contributions: Study conception and design, and manuscript preparation: S.S. and R.F.M.; data acquisition: S.S., J.R.S., B.D., and N.J.; analysis and interpretation: S.S., J.C., and R.F.M.

Correspondence and requests for reprints should be addressed to Roberto F. Machado, M.D., 909 S. Wolcott Avenue, 3108 COMRB (MC719), Chicago, IL 60612. E-mail: machador@uic.edu

Am J Respir Cell Mol Biol Vol 57, Iss 3, pp 307–314, Sep 2017

Originally Published in Press as DOI: 10.1165/rcmb.2016-0287OC on April 19, 2017
Internet address: www.atsjournals.org

Hemin-TLR4 signaling and the pro-oxidant effects of hemin on ECs may contribute to endothelial barrier dysfunction during ACS, since both TLR4 and ROS are well-known mediators of EC barrier disruption by a number of different mechanisms (10–12). The EC barrier is maintained by junctional proteins and peripheral actin fibers that serve to optimize cell–cell and cell–matrix contact (13). EC barrier disruption in response to various bioactive stimuli is often characterized by a rearrangement of actin from peripheral locations into transcellular, contractile actomyosin stress fibers that pull apart cell–cell junctions, leading to the formation of paracellular gaps (13). TLR4 signaling and ROS are known to promote intercellular gap formation by direct effects on junctional proteins as well as actin filament organization, and are also involved in a number of different signaling pathways known to promote actin cytoskeletal rearrangements that favor increased EC permeability (11, 12, 14, 15). For example, ECs that sustain oxidative stress have been shown to display increased intracellular $Ca^{2+}$ levels associated with enhanced myosin light chain phosphorylation, a key molecular event that leads to the aforementioned actomyosin contraction and consequent increase in EC permeability (16, 17). Finally, ROS may enhance pulmonary vascular leak by promoting EC cell death, as has been observed in a sepsis-induced rodent model of acute lung injury (18).

In the current study, we hypothesized that hemin exerts barrier-disruptive effects on lung microvascular ECs via TLR4 signaling and the promotion of oxidant stress.

## Materials and Methods

### Reagents

Hemin, purchased from Sigma-Aldrich (St. Louis, MO), was prepared as previously described (6). Briefly, hemin powder was dissolved in 0.25 M NaOH and the pH was increased to 7.4 with the addition of HCl. Then, PBS was added to bring the solution to the desired final concentration. Fluorescein isothiocyanate (FITC)-labeled dextran (3 kD) and *N*-acetyl-L-cysteine were purchased from Sigma-Aldrich and diluted to the desired concentration in endothelial basal media (EBM-2; Lonza, Basel, Switzerland). TAK-242, z-vad-fmk, 2′,7′-dichlorofluorescein diacetate (DCFDA), and necrostatin-1 were also obtained from Sigma-Aldrich. Concentrated stock solutions prepared in DMSO were subsequently diluted to the desired concentration in endothelial basal media such that the final concentration of DMSO was less than 0.1% of the total media volume used in cell culture experiments. Human lung microvascular ECs (hLMVECs; cat.# CC-2257), EC growth media, and 0.4% Trypan blue solution were purchased from Lonza. Anti–phosphorylated mixed lineage kinase domain-like protein (anti-phospho-MLKL; cat.# ab187091) and anti-cleaved-caspase-3 antibodies (cat.# 9664) were obtained from Abcam (Cambridge, UK) and Cell Signaling (Danvers, MA), respectively.

### Cell Culture

hLMVECs obtained from Lonza were grown in cell culture using endothelial growth media containing supplemental growth factors and 5% fetal bovine serum according to the manufacturer's instructions. Cells underwent a maximum of three passages for use in experiments. In all experiments, complete growth media was removed and replaced with basal media (without serum or growth factors) 3 h before hemin treatment.

### Electric Cell Impedance Sensing Permeability Assay

ECs were grown to confluence in polycarbonate wells containing evaporated gold microelectrodes purchased from Applied BioPhysics (Troy, NY), and measurements of transendothelial electrical resistance (TER) were performed using an electric cell impedance sensing (ECIS) system (Applied BioPhysics) as described previously (19–21). Briefly, a 4,000-Hz alternating current was applied across the electrodes with a fixed amplitude and external resistance to establish a constant current of ~1 μA. The in-phase and out-of-phase voltages between the electrodes were measured in real time and used to calculate the TER. Increased cell adherence and confluence correlates with a higher TER, whereas cell retraction, rounding, or loss of adhesion leads to a decrease in TER (22). TER was monitored for stability before hemin treatment was initiated in all experiments, and a threshold of 2.5 × 103 Ω was required for hLMVECs to be considered confluent on the electrodes and suitable for study. The TER from each microelectrode was measured at discrete time intervals and recorded for analysis.

### FITC-Dextran Transwell Permeability Assay

ECs were grown to confluency on Transwell inserts (EMD Millipore, Kankakee, IL) containing 3 μm pores. Then, 10 μg/ml of FITC-labeled dextran (3 kD) was added to the media over the cells along with either vehicle or 40 μM of hemin. After 30 min, 100 μl of media was extracted from below the Transwell insert for measurement of FITC concentration by fluorometry (with excitation and emission spectrum peak wavelengths of 495 nm and 519 nm, respectively) to determine the degree of EC monolayer permeability in either condition, as described previously (23).

### Trypan Blue Staining

hLMVECs treated with hemin versus vehicle were washed with PBS and treated with 0.05% trypsin for removal into a buffered saline suspension. Then, 0.4% Trypan blue was added to the suspension in a 1:1 dilution, and an aliquot of the diluted suspension was used to fill a hemocytometer chamber. Stained versus unstained cells were counted manually under a light microscope in 10 high-powered fields for each replicate of the two experimental conditions.

### Terminal Deoxynucleotidyl Transferase dUTP Nick-End Labeling Assay

hLMVECs were grown in 96-well plates and pretreated with 1 mM N-acetylcysteine (NAC) for 3 h and/or 400 nM TAK-242 for 1 h before treatment with 40 μM hemin for 30 min. *In situ* detection of DNA fragmentation by terminal deoxynucleotidyl transferase (TdT) nick-end labeling (TUNEL) with biotinylated nucleotides was performed using the TiterTACS Colorimetric Apoptosis Detection Kit (Trevigen, Gaithersburg, MD) in accordance with the manufacturer's instructions. Briefly, cells were fixed with 3.7% buffered formaldehyde, followed by permeabilization with methanol and cytonin. Positive controls were treated with TACS-Nuclease. Endogenous peroxidase was quenched with peroxide before TdT labeling with biotinylated dUTPs. After washing, the cells were then incubated with a streptavidin-horseradish peroxidase

solution, and a colorimetric readout was obtained after addition of the appropriate horseradish peroxidase substrates, with absorbance measured at 450 nm.

### Western Blotting

hLMVECs were grown in 6-well plates and pretreated with 1 mM NAC for 3 h and/or 400 nM TAK-242 for 1 h before treatment with 40 μM hemin for 30 min. After 30 min, cells were washed with ice-cold PBS and scraped off of the plate in RIPA buffer containing protease and phosphatase inhibitor cocktails. After addition of Laemmli buffer, samples were boiled for 10 min and loaded into separate lanes of a 10% TGX (Tris/glycine extended) gel. This is a proprietary precast gel made by Bio-rad Laboratories (Des Plaines, IL) using a modification of the Laemmli system that results in increased gel matrix stability and shelf life but retains Laemmli-like separation properties. After SDS-PAGE and transfer of gel onto nitrocellulose membranes, Western blotting was performed using anti-phospho-MLKL and anti-cleaved-caspase-3 antibodies according to the manufacturer's instructions. A positive control for caspase-3 antibody was prepared using lysate from A549 cells treated with TNF-α.

### DCFDA Cellular ROS Detection and Measurement

hLMVECs were grown to confluence in 96-well plates. They were then incubated in serum-free basal media containing 25 μM DCFDA for 45 min, and subsequently washed with PBS before incubation with DMSO/necrostatin-1 and/or PBS/hemin. Fluorescence was measured in a plate reader using an excitation wavelength of 485 nm and an emission wavelength of 535 nm.

### Statistical Analysis

A two-tailed Student's *t* test was performed on all data using Microsoft Excel (*$P < 0.05$).

## Results

### Assessment of the Effects of Hemin on the *Trans*-Monolayer Resistance of hLMVECs

hLMVECs were grown to confluency on gold electrodes and subjected to ECIS assessments of TER in response to varying concentrations of hemin ranging from 5 to 100 μM. As shown in Figure 1, increasing concentrations of hemin resulted in increasingly larger decreases in TER over the course of the experiment, with substantial and sustained decrements occurring at concentrations of 40 μM and higher. Marginal decreases in TER were observed at concentrations lower than this threshold (20 and 30 μM; Figure 1B), which recovered to baseline gradually over several hours.

Because there was no recovery in TER even after 20 h of observations when the ECs were exposed to concentrations of 40 μM and higher, we hypothesized that cell death was occurring in response to hemin. We also thought that the extremely gradual recovery in the marginal TER decrement seen at the 20 and 30 μM concentrations was related to regeneration of the monolayer at lower levels of hemin-induced cell death, since the time course of recovery was compatible with cellular expansion. We therefore chose to use a concentration of 40 μM to study the appreciable effects of hemin on hLMVEC permeability in all subsequent experiments.

### Assessment of *Trans*-Monolayer FITC-Dextran Flux

To confirm that the observed decreases in TER in response to hemin correlated with increased permeability of the EC monolayer, we performed an assessment of *trans*-monolayer FITC-dextran flux. hLMVECs were grown to confluency on Transwell inserts containing 3 μm pores, and then treated with 10 μg/ml FITC-dextran (3 kD) added to the media overlying the monolayer. After exposure to either PBS or 40 μM hemin for 30 min, media from the chamber underlying the Transwell inserts was extracted for fluorometry. As shown in Figure 1C, hemin exposure resulted in

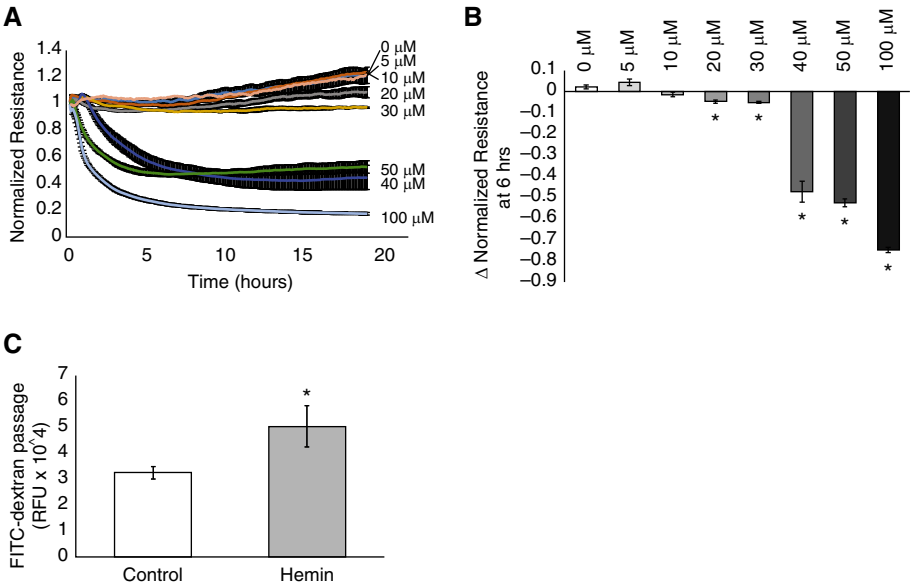


**Figure 1.** Hemin decreases the transendothelial electrical resistance (TER) of a human lung microvascular endothelial cell (hLMVEC) monolayer in a concentration-dependent manner and increases fluorescein isothiocyanate (FITC)-dextran passage. hLMVECs were grown to confluency on gold electrodes. Resistance to an electrical current applied to the electrode was measured and used as a marker for the degree of barrier-enhancing cell–cell attachment after treatment with varying concentrations of hemin (100 μM, 50 μM, 40 μM, 30 μM, 20 μM, 10 μM, and 5 μM) versus vehicle-treated controls. The plot in *A* depicts the average electrical resistance normalized to baseline resistance over time after hemin treatment in $n = 3$ experiments. Hemin was added at time 0. *Error bars* are ± SD. The *bar graph* in *B* shows the maximal percent decrease in resistance after 6 h of hemin exposure versus hemin concentration/vehicle-treated controls. In separate experiments, hLMVECs were grown to confluency on Transwell inserts with 3 μm pores in media that contained 3 kD FITC-dextran. After treatment with either vehicle control or 40 μM hemin, media from below the monolayer was sampled and analyzed by fluorometry for the presence of FITC-dextran. The *bar graph* in *C* depicts the relative fluorescence units (RFU) of media taken from below control versus hemin-treated monolayers in $n = 3$ experiments. *Error bars* are ± SD. *Indicates significant difference from control (Student's *t* test, $P < 0.05$).

increased *trans*-monolayer flux of FITC-dextran relative to PBS-treated control monolayers.

### Assessment of the Role of TLR4 and Oxidative Stress

We next sought to determine the role of hemin-TLR4 signaling, as well as the pro-oxidant characteristics of hemin, in the observed effects on the EC monolayer TER. hLMVECs were again grown to confluency on gold electrodes for ECIS assessment of TER and pretreated with a 400 nM concentration of the TLR4 inhibitor, TAK-242, for 1 h before addition of hemin and/or an antioxidant (1 mM NAC) for 3 h before exposure to 40 μM hemin. As shown in Figure 2, both 400 nM TAK-242 and 1 mM NAC abrogated the effects of hemin on the TER. Pretreatment with both agents did not result in any statistically significant greater abrogation compared with TAK-242 alone.

### Assessment of the Role of Iron

We then examined the potential role of iron in the effects of hemin on EC barrier function. hLMVECs grown to confluency on gold electrodes were pretreated with a 1 μM concentration of the iron chelator deferoxamine 1 h before hemin exposure. As shown in Figure 3, deferoxamine pretreatment largely abrogated the effects of hemin on the EC TER.

### Hemin Induces Programmed EC Death, as Evidenced by Trypan Blue Staining and TUNEL Assay

To determine whether cell death was occurring in hLMVECs exposed to hemin, we performed Trypan blue staining on control versus hemin-treated hLMVECs. ECs were grown in 6-well plates and treated with either PBS or hemin for 30 min, after which they were trypsinized and stained with Trypan blue while in suspension. Trypan-blue–positive cells were observed under a light microscope and counted manually. Figure 4A displays a representative field of cells observed in the hemin-treated group, and a marked increase in nonviable cells is shown in Figure 4B. Because hemin has been shown to cause programmed cell death of other cell types (24–27), we performed a TUNEL assay to determine whether programmed cell death is part of the mechanism of hemin-induced cell death. We also pretreated cells with TAK-242 or NAC to confirm that the abrogation of TER

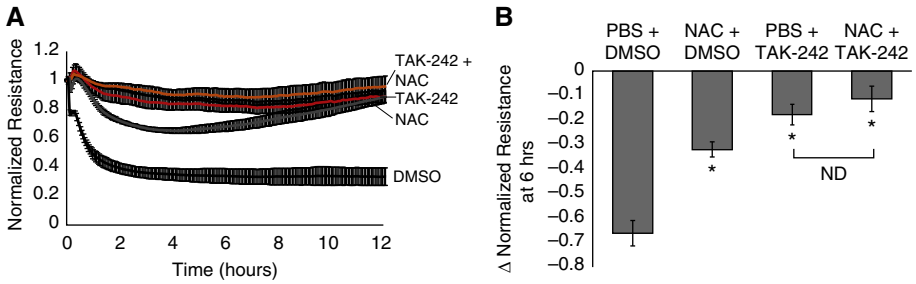


**Figure 2.** Pretreatment with the Toll-like receptor 4 (TLR4) inhibitor TAK-242 and/or the antioxidant N-acetylcysteine (NAC) abrogates hemin-induced decreases in TER. hLMVECs grown on gold electrodes for electric cell impedance sensing (ECIS) assessment of TER were pretreated with 1 mM NAC versus PBS vehicle for 3 h before 40 μM hemin treatment and/or 400 nM TAK-242 versus DMSO vehicle for 1 h before hemin exposure. The plot in *A* depicts the average electrical resistance normalized to baseline resistance over time after hemin treatment in $n = 3$ experiments. Hemin was added at time 0. *Error bars* are ± SD. The *bar graph* in *B* shows the maximal percent decrease in resistance after 6 h of hemin treatment in vehicles/hemin, TAK-242/hemin, NAC/hemin, and TAK-242/NAC/hemin treatment groups. *Error bars* are ± SD. *Indicates significant difference from control (Student's *t* test, $P < 0.05$). ND, not detected.

decrements by these agents is due to a central role of hemin-TLR4 signaling and oxidant stress in programmed cell death. As shown in Figure 4C, hemin treatment resulted in increased DNA fragmentation usually associated with programmed cell death, and this effect was largely abrogated by deferoxamine, TAK-242, or NAC pretreatment, indicating that hemin-TLR4 signaling and ROS are key components of the mechanism.

### Hemin Causes Necroptosis and Not Apoptosis of ECs via Hemin-TLR4 Signaling and Oxidant Stress

We performed Western blotting for key effectors of programmed cell death to determine the pathway involved in hemin-induced effects on hLMVECs. We first probed for activation of the final common effector caspase of both the extrinsic and intrinsic apoptotic pathways using an antibody against cleaved caspase-3 (28). We did not find any evidence of caspase-3 activation by hemin (Figure 5). Consistent with what is now known about caspase-independent programmed cell death, which may be triggered by TLR4 (29) and/or oxidant stress (30) and may result in TUNEL positivity (31), we hypothesized that necroptosis is the major pathway involved in hemin-induced cell death. We therefore probed for the presence of phospho-MLKL, which is directly responsible for the disruption of intracellular and plasma membranes as a key effector of necroptosis (32). MLKL is activated by RIP3 kinase-mediated

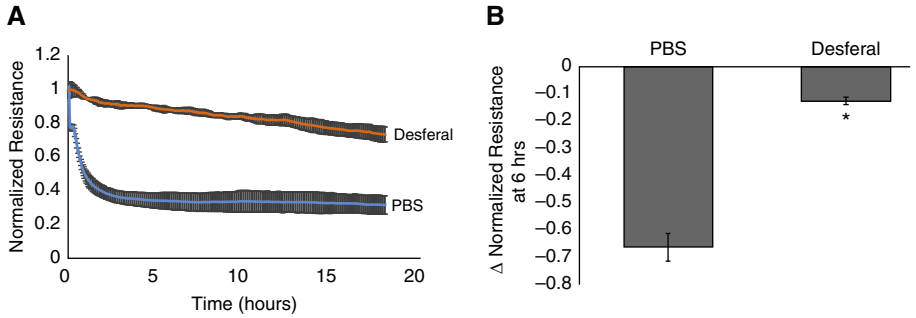


**Figure 3.** Pretreatment with the iron chelator deferoxamine abrogates hemin-induced decreases in TER. hLMVECs grown on gold electrodes for ECIS assessment of TER were pretreated with 1 μM deferoxamine versus PBS vehicle for 1 h before 40 μM hemin exposure. The plot in *A* depicts the average electrical resistance normalized to baseline resistance over time after hemin treatment in $n = 3$ experiments. Hemin was added at time 0. *Error bars* are ± SD. The *bar graph* in *B* shows the maximal percent decrease in resistance after 6 h of hemin treatment in both groups. *Error bars* are ± SD. *Indicates significant difference from control (Student's *t* test, $P < 0.05$).

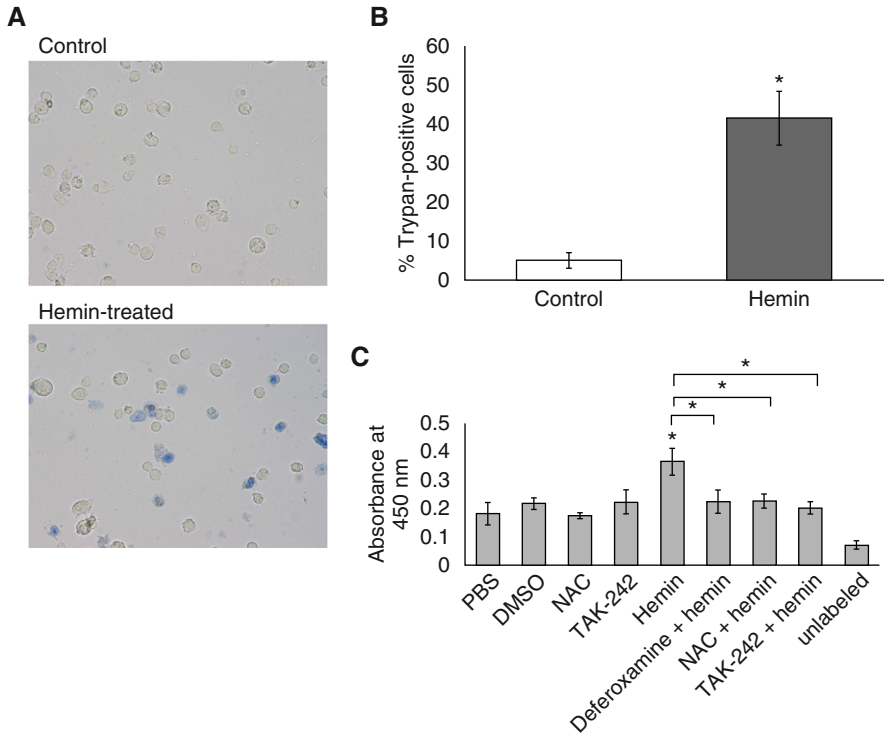


**Figure 4.** Treatment with 40 μM hemin causes programmed hLMVEC death. hLMVECs grown to confluence in 6-well plates were treated with either vehicle or 40 μM hemin. Cells were trypsinized and stained with Trypan blue. Aliquots of the stained cell suspensions were placed in a hemocytometer chamber on a slide and visualized under 20× magnification with a light microscope. Representative fields for each condition are shown in *A*. In *B*, the *bar graph* depicts the average percentage of Trypan-blue–positive cells in 10 high-powered fields for control versus hemin-treated groups. In separate experiments, hLMVECs were grown in 96-well plates and treated with 400 nM TAK-242 and/or 1 mM NAC or 1 μM deferoxamine versus vehicle controls + 40 μM hemin. DNA fragmentation was detected *in situ* by TdT nick-end labeling with biotinylated nucleotides, followed by secondary labeling with streptavidin-horseradish peroxidase and incubation with peroxidase substrates, resulting in a colorimetric readout quantified by spectrophotometric absorbance at 450 nm. The *bar graph* in *C* depicts the average relative absorbances of the various treatment conditions. *Error bars* are ± SD. *Indicates significant difference from control (Student's *t* test, $P < 0.05$).

phosphorylation at T357/S358 (31–33). Using an antibody specific for phospho-MLKL (S358), we found evidence of necroptosis in hemin-treated ECs, as shown in Figure 5. NAC or TAK-242 pretreatment abrogated MLKL activation, suggesting a central role for hemin-TLR4 and oxidant stress in activation of necroptosis.

To confirm that cell death was due to necroptosis and not apoptosis, we repeated the ECIS experiment and TUNEL assay utilizing specific inhibitors for these pathways. As shown in Figure 6, pretreatment of hLMVECs with 50 μM necrostatin-1 abrogated hemin-induced decrements in TER and the degree of DNA fragmentation detected by TUNEL. On the other hand, the pan-caspase inhibitor z-vad-fmk had little to no effect on either parameter. To determine whether inhibition of necroptosis had any effect on hemin-induced ROS production, we measured ROS DCFDA fluorescence in hemin-treated versus necrostatin-1+hemin–treated hLMVECs. As shown in Figure 6D, there was no significant difference in ROS production between these two groups.

## Discussion

A role for endothelial barrier dysfunction during ACS has been suggested by the observed progression to ARDS in a fraction of ACS cases (5). Furthermore, in a murine model of SCD that closely recapitulates the longitudinal morbidities and mortality characteristics of human disease, Ghosh and colleagues recently described long-term vascular inflammation, endothelial injury, and pulmonary vascular leak in this disease (34). In the current study, we discovered that one of the key mediators of ACS, hemin, has the potential to cause endothelial barrier dysfunction by directing necroptotic programmed EC death via hemin-TLR4 signaling and cellular oxidant stress. TLR4 is a known signaling trigger for necroptosis, as is ROS (35, 36). It is also known that TLR4 lies upstream of ROS (37), and our data are consistent with that finding because the addition of NAC to the TLR4 inhibitor TAK-242 did not result in any statistically significant greater abrogation of hemin-induced necroptosis or barrier dysfunction compared with TAK-242 alone. Similar vascular endothelial injury by programmed cell death has been observed in animal models of other forms of ARDS, but its role in human cases of the syndrome remains unclear (38). Interestingly, it was also observed in a study in which hLMVECs were exposed to stored human red blood cells (RBCs) and subsequently underwent necroptosis (39). A follow-up examination of the blood of critically ill human patients receiving transfusions of stored RBCs revealed increased levels of RIP3 as evidence of *in vivo* transfusion-induced necroptosis (39). It remains unclear from that study how the RBCs triggered necroptosis, but increased oxidant stress in association with the phenomenon was noted (39).

Our observations of hemin-induced necroptosis are consistent with previous findings in at least one other study. Laird and colleagues reported that in an *in vitro* model of intracranial hemorrhage, mouse cortical astrocytes exposed to hemin in culture underwent necroptosis in a concentration-dependent manner (25). Interestingly, necroptosis was dependent on preceding inflammatory gene expression and ROS production, and either inhibition of NfkB or antioxidant pretreatment with NAC attenuated cell death (25). Some of these characteristic effects of hemin are consistent with what was previously described in endothelial cells by Belcher and colleagues (9). In their study, hemin activated NfkB via TLR4 signaling, resulting in inflammatory gene expression that included VCAM-1, P-selectin, E-selectin, IL-1, IL-6, IL-8, and tissue factor

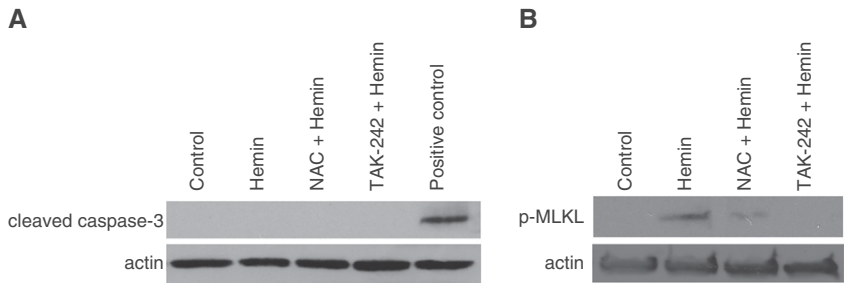


**Figure 5.** Addition of 40 μM hemin causes caspase-3–independent necroptosis that is abrogated by either TAK-242 or NAC pretreatment. hLMVECs were grown in 6-well plates and treated with 40 μM hemin ± 1 mM NAC. Cell lysates from three replicates of each condition were subjected to SDS-PAGE and transferred to nitrocellulose membranes for Western blotting. Shown are representative blots for (*A*) cleaved caspase-3 and (*B*) phospho-MLKL (S358). MLKL, mixed lineage kinase domain-like pseudokinase.

(9). In parallel, hemin-TLR4 was also observed to induce a protein kinase C-dependent activation of endothelial NADPH oxidase, resulting in ROS-mediated Weibel-Palade degranulation (9). However, no cell death was described in their study in relation to either hemin-related NfkB activation or oxidative stress.

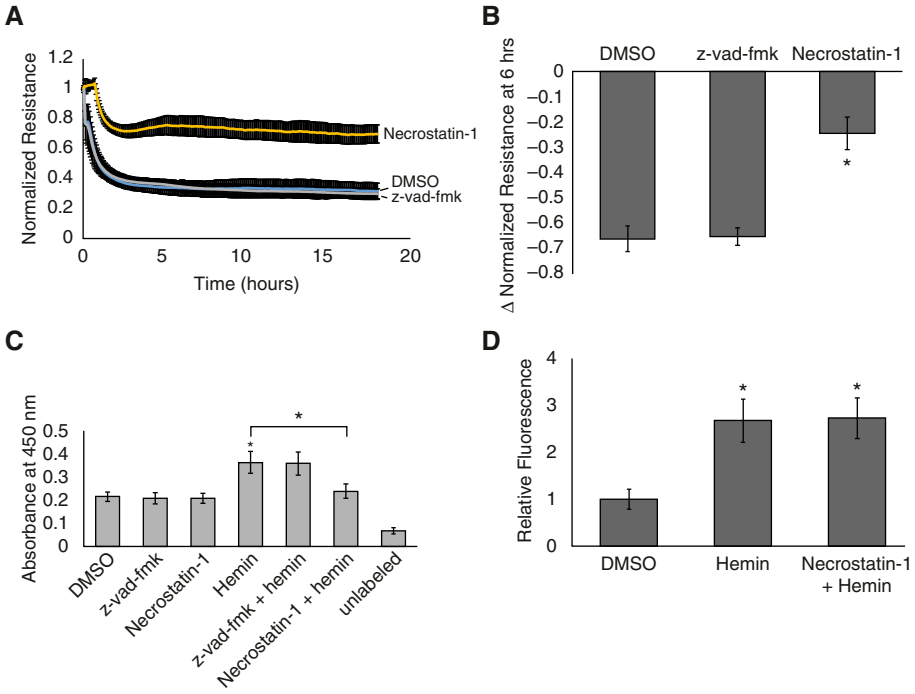


**Figure 6.** Necrostatin-1, but not z-vad-fmk, abrogates hemin-induced barrier dysfunction and cell death. To confirm that hemin-induced cell death occurred via necroptosis and not apoptosis, ECIS studies and TUNEL assays were repeated after pretreatment of cells with either 50 μM necrostatin-1 or 10 μM z-vad-fmk for 1 h before 40 μM hemin exposure. (*A*) Average electrical resistance normalized to baseline resistance over time after hemin treatment in $n = 3$ experiments. Hemin was added at time 0. *Error bars* are ± SD. The *bar graph* in *B* shows the maximal percent decrease in resistance after 6 h of hemin treatment in both groups. (*C*) Results of the TUNEL assay in $n = 3$ experiments. *Error bars* are ± SD. (*D*) hLMVECs grown in 96-well plates and stained with 25 μM dichlorofluorescein diacetate were treated with either DMSO or 50 μM necrostatin-1 for 1 h before exposure to 40 μM hemin. Within 5 min of hemin treatment, fluorescence was measured using an excitation wavelength of 485 nm and an emission wavelength of 535 nm as a measure of reactive oxygen species (ROS) production. The *bar graph* depicts the fold increase in fluorescence relative to DMSO+PBS–treated cells in $n = 3$ experiments. *Error bars* are ± SD. *Indicates significant difference from control (Student's *t* test, $P < 0.05$).

The reasons for this discrepancy are unclear, but it may be related to either the specific cell type studied or the concentration of hemin used. In the aforementioned study, 20 μM hemin was used in human umbilical vein ECs, whereas we observed that cell death occurred at concentrations greater than 40 μM in hLMVECs. Notwithstanding the well-known heterogeneity of EC responses, which vary by tissue type and even intratissue location (e.g., macro- versus microvascular) (40–42), the higher concentration of hemin used in our study is likely a key factor underlying the observed presence of cell death versus the inflammation and EC activation without cell death observed by Belcher and colleagues (9).

On the other hand, a handful of published studies have demonstrated endothelial barrier–protective, anti-inflammatory, and antiapoptotic properties associated with hemin pretreatment and its resultant preactivation of tissue heme oxygenase-1, a stress-responsive antioxidant enzyme (43–45). It would appear that concentrations of hemin similar to or higher than what we used in our current study were observed to have endothelial-protective effects in these studies, directly contradicting our findings. However, a key difference between the published studies and ours is that all of the prior studies were conducted under conditions that did not necessarily reproduce the sickle cell–related microenvironment, i.e., they were performed in the presence of normal levels of hemin-binding proteins. Patients with SCD are known to be deficient in heme-binding proteins such as hemopexin and haptoglobin (6, 46, 47). It was previously shown that infusion of extracellular hemin does not cause ACS/endothelial barrier dysfunction in wild-type mice as it does in sickle cell mice (6). Sickle cell mice that are otherwise deficient in blood hemopexin can be protected from the effects of hemin by pretreatment with hemopexin (6). In the current study, we performed all experiments under serum-free conditions (*see* Materials and Methods) so as to mimic the deficiency of heme-binding proteins of SCD, and under these conditions, hemin-TLR4–induced necroptosis of LMVECs predominated. In contrast, in the studies cited above, the experiments were performed either in ECs maintained with serum-containing medium

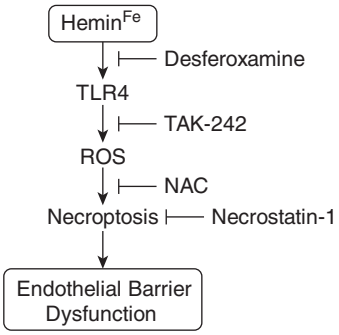


**Figure 7.** Hemin causes lung microvascular endothelial barrier dysfunction by necroptotic cell death. Hemolytic events during sickle cell crises increase free hemin levels in the blood. The iron moiety of hemin is required for hemin-TLR4 signaling to take place in microvascular endothelial cells. ROS generation is depicted as being downstream of hemin-TLR4, because the addition of NAC to TAK-242 did not result in any greater abrogation of barrier dysfunction (Figure 2), and the literature (9) suggests that ROS generation in endothelial cells exposed to hemin is TLR4 dependent. ROS results in triggering of necroptosis and consequent barrier dysfunction.

or in wild-type animals, where the heme oxygenase–inducing properties of hemin predominated and resulted in subsequent protection from barrier dysfunction, inflammation, and cell death in response to a variety of other stimuli (43–45). Therefore, we believe our observations are more specifically relevant to the development of novel therapies targeting microvascular barrier dysfunction and the consequent morbidity-producing, noncardiogenic pulmonary edema that occurs during ACS in patients with SCD.

At steady state, baseline plasma heme concentrations in patients with SCD have been found to average ~4 μM, with the highest concentrations nearing 20 μM (48). On the other hand, the precise amount of free extracellular hemin circulating in the blood of SCD patients during the vaso-occlusive crises preceding ACS is currently unknown. However, it is worth noting that in the Cooperative Study of Sickle Cell Disease, which included 1,722 episodes of ACS observed in 939 patients, severe acute hemolysis that potentially could have increased extracellular hemoglobin by 3.6 g/dl was revealed to predict sudden death (4, 6). This amount of free hemoglobin would be roughly equivalent to 2.23 mM hemin, assuming 100% heme release and auto-oxidation (6). The concentration of hemin used in our study is less than 2% of that amount, and therefore certainly within the realm of possible hemin concentrations present in the sickest of patients with ACS. It is also worth noting that in their description of hemin infusion as a rodent model for ACS, Ghosh and colleagues induced more than 10 times the blood concentration of hemin (0.43 mM) as what resulted in EC necroptosis and consequent barrier dysfunction in our study, and in their model, 70% of sickle cell mice receiving this amount of hemin developed lethal ARDS (6).

In addition to necroptotic cell death, it is certainly possible that hemin exerts additional effects on adherens and tight-junction proteins. Because hemin signals through TLR4 in ECs, it could lead to phosphorylation of VE-Cadherin (15) and/or occludin (12), thereby opening adherens or tight junctions, or both, to increase paracellular permeability. However, at the concentration of hemin used in our study, at least 40–50% of the cells were observed to undergo programmed cell death, making cell death the predominant phenomenon studied further in this paper. Whether an additional background phenomenon of increased paracellular permeability via phosphorylation of junctional protein(s) contributed to the observed barrier dysfunction is a challenging question to answer within the scope of the current study and in the context of such extensive cell death. Nevertheless, this may be worth studying in the future as a possible mechanism of increased permeability at lower concentrations of hemin or during inhibition of hemin-induced necroptosis.

## Conclusions

In summary, we observed significant endothelial barrier dysfunction in response to hemin exposure that appears to be due to TLR4- and oxidant-stress–mediated necroptosis (Figure 7). Given the mounting data supporting the relevance of necroptosis during critical illnesses (49), as well as the emerging importance of hemin in the pathogenesis of ACS, we believe that our observations reveal a highly relevant component of the mechanisms underlying this disease. Further studies examining the role of EC necroptosis in promoting noncardiogenic pulmonary edema during ACS are warranted, and may open a new avenue of potential treatments for this devastating disease. ■

**Author disclosures** are available with the text of this article at www.atsjournals.org.

## References

1. Platt OS, Brambilla DJ, Rosse WF, Milner PF, Castro O, Steinberg MH, Klug PP. Mortality in sickle cell disease. Life expectancy and risk factors for early death. *N Engl J Med* 1994;330:1639–1644.
2. Ballas SK, Lieff S, Benjamin LJ, Dampier CD, Heeney MM, Hoppe C, Johnson CS, Rogers ZR, Smith-Whitley K, Wang WC, *et al.*; Investigators, Comprehensive Sickle Cell Centers. Definitions of the phenotypic manifestations of sickle cell disease. *Am J Hematol* 2010;85:6–13.
3. Vichinsky EP, Neumayr LD, Earles AN, Williams R, Lennette ET, Dean D, Nickerson B, Orringer E, McKie V, Bellevue R, *et al.*; National Acute Chest Syndrome Study Group. Causes and outcomes of the acute chest syndrome in sickle cell disease. *N Engl J Med* 2000;342:1855–1865.
4. Vichinsky EP, Styles LA, Colangelo LH, Wright EC, Castro O, Nickerson B; Cooperative Study of Sickle Cell Disease. Acute chest syndrome in sickle cell disease: clinical presentation and course. *Blood* 1997;89:1787–1792.
5. Haynes J Jr, Allison RC. Pulmonary edema. Complication in the management of sickle cell pain crisis. *Am J Med* 1986;80:833–840.
6. Ghosh S, Adisa OA, Chappa P, Tan F, Jackson KA, Archer DR, Ofori-Acquah SF. Extracellular hemin crisis triggers acute chest syndrome in sickle mice. *J Clin Invest* 2013;123:4809–4820.
7. Hebbel RP, Morgan WT, Eaton JW, Hedlund BE. Accelerated autoxidation and heme loss due to instability of sickle hemoglobin. *Proc Natl Acad Sci USA* 1988;85:237–241.
8. Liu SC, Zhai S, Palek J. Detection of hemin release during hemoglobin S denaturation. *Blood* 1988;71:1755–1758.
9. Belcher JD, Chen C, Nguyen J, Milbauer L, Abdulla F, Alayash AI, Smith A, Nath KA, Hebbel RP, Vercellotti GM. Heme triggers TLR4 signaling leading to endothelial cell activation and vaso-occlusion in murine sickle cell disease. *Blood* 2014;123:377–390.
10. Boueiz A, Hassoun PM. Regulation of endothelial barrier function by reactive oxygen and nitrogen species. *Microvasc Res* 2009;77:26–34.
11. Sukriti S, Tauseef M, Yazbeck P, Mehta D. Mechanisms regulating endothelial permeability. *Pulm Circ* 2014;4:535–551.

12. Vandenbroucke E, Mehta D, Minshall R, Malik AB. Regulation of endothelial junctional permeability. *Ann N Y Acad Sci* 2008;1123: 134–145.
13. Garcia JG, Schaphorst KL. Regulation of endothelial cell gap formation and paracellular permeability. *J Investig Med* 1995;43: 117–126.
14. Lum H, Roebuck KA. Oxidant stress and endothelial cell dysfunction. *Am J Physiol Cell Physiol* 2001;280:C719–C741.
15. Gong P, Angelini DJ, Yang S, Xia G, Cross AS, Mann D, Bannerman DD, Vogel SN, Goldblum SE. TLR4 signaling is coupled to SRC family kinase activation, tyrosine phosphorylation of zonula adherens proteins, and opening of the paracellular pathway in human lung microvascular endothelia. *J Biol Chem* 2008;283: 13437–13449.
16. Elliott SJ, Meszaros JG, Schilling WP. Effect of oxidant stress on calcium signaling in vascular endothelial cells. *Free Radic Biol Med* 1992;13:635–650.
17. Zhao Y, Davis HW. Hydrogen peroxide-induced cytoskeletal rearrangement in cultured pulmonary endothelial cells. *J Cell Physiol* 1998;174:370–379.
18. Gill SE, Rohan M, Mehta S. Role of pulmonary microvascular endothelial cell apoptosis in murine sepsis-induced lung injury in vivo. *Respir Res* 2015;16:109.
19. Garcia JG, Schaphorst KL, Shi S, Verin AD, Hart CM, Callahan KS, Patterson CE. Mechanisms of ionomycin-induced endothelial cell barrier dysfunction. *Am J Physiol* 1997;273:L172–L184.
20. Giaever I, Keese CR. A morphological biosensor for mammalian cells. *Nature* 1993;366:591–592.
21. Tiruppathi C, Malik AB, Del Vecchio PJ, Keese CR, Giaever I. Electrical method for detection of endothelial cell shape change in real time: assessment of endothelial barrier function. *Proc Natl Acad Sci USA* 1992;89:7919–7923.
22. Garcia JG, Schaphorst KL, Verin AD, Vepa S, Patterson CE, Natarajan V. Diperoxovanadate alters endothelial cell focal contacts and barrier function: role of tyrosine phosphorylation. *J Appl Physiol (1985)* 2000;89:2333–2343.
23. Martins-Green M, Petreaca M, Yao M. An assay system for in vitro detection of permeability in human "endothelium". *Methods Enzymol* 2008;443:137–153.
24. Higdon AN, Benavides GA, Chacko BK, Ouyang X, Johnson MS, Landar A, Zhang J, Darley-Usmar VM. Hemin causes mitochondrial dysfunction in endothelial cells through promoting lipid peroxidation: the protective role of autophagy. *Am J Physiol Heart Circ Physiol* 2012;302:H1394–H1409.
25. Laird MD, Wakade C, Alleyne CH Jr, Dhandapani KM. Hemin-induced necroptosis involves glutathione depletion in mouse astrocytes. *Free Radic Biol Med* 2008;45:1103–1114.
26. Levy YS, Streifler JY, Panet H, Melamed E, Offen D. Hemin-induced apoptosis in PC12 and neuroblastoma cells: implications for local neuronal death associated with intracerebral hemorrhage. *Neurotox Res* 2002;4:609–616.
27. Sukumari-Ramesh S, Laird MD, Singh N, Vender JR, Alleyne CH Jr, Dhandapani KM. Astrocyte-derived glutathione attenuates hemin-induced apoptosis in cerebral microvascular cells. *Glia* 2010; 58:1858–1870.
28. Porter AG, Jänicke RU. Emerging roles of caspase-3 in apoptosis. *Cell Death Differ* 1999;6:99–104.
29. Silke J, Rickard JA, Gerlic M. The diverse role of RIP kinases in necroptosis and inflammation. *Nat Immunol* 2015;16: 689–697.
30. Shindo R, Kakehashi H, Okumura K, Kumagai Y, Nakano H. Critical contribution of oxidative stress to TNFα-induced necroptosis downstream of RIPK1 activation. *Biochem Biophys Res Commun* 2013;436:212–216.
31. Zhou W, Yuan J. SnapShot: necroptosis. *Cell* 2014;158:464–464.e1.
32. Pasparakis M, Vandenabeele P. Necroptosis and its role in inflammation. *Nature* 2015;517:311–320.
33. Linkermann A, Green DR. Necroptosis. *N Engl J Med* 2014;370:455–465.
34. Ghosh S, Ihunnah CA, Hazra R, Walker AL, Hansen JM, Archer DR, Owusu-Ansah AT, Ofori-Acquah SF. Nonhematopoietic Nrf2 dominantly impedes adult progression of sickle cell anemia in mice. *JCI Insight* 2016;1:e81090.
35. Fulda S. Regulation of necroptosis signaling and cell death by reactive oxygen species. *Biol Chem* 2016;397:657–660.
36. He S, Liang Y, Shao F, Wang X. Toll-like receptors activate programmed necrosis in macrophages through a receptor-interacting kinase-3-mediated pathway. *Proc Natl Acad Sci USA* 2011;108:20054–20059.
37. Asehnoune K, Strassheim D, Mitra S, Kim JY, Abraham E. Involvement of reactive oxygen species in Toll-like receptor 4-dependent activation of NF-kappa B. *J Immunol* 2004;172:2522–2529.
38. Matute-Bello G, Martin TR. Apoptosis in the pathogenesis and resolution of acute lung injury. In: Choi AMK, editor. Acute respiratory distress syndrome, 2nd ed. New York: Informa Healthcare USA, Inc.; 2009. pp. 93–108.
39. Qing DY, Conegliano D, Shashaty MG, Seo J, Reilly JP, Worthen GS, Huh D, Meyer NJ, Mangalmurti NS. Red blood cells induce necroptosis of lung endothelial cells and increase susceptibility to lung inflammation. *Am J Respir Crit Care Med* 2014;190:1243–1254.
40. Garlanda C, Dejana E. Heterogeneity of endothelial cells. Specific markers. *Arterioscler Thromb Vasc Biol* 1997;17:1193–1202.
41. Muth H, Maus U, Wygrecka M, Lohmeyer J, Grimminger F, Seeger W, Günther A. Pro- and antifibrinolytic properties of human pulmonary microvascular versus artery endothelial cells: impact of endotoxin and tumor necrosis factor-α. *Crit Care Med* 2004;32:217–226.
42. Shelton JL, Wang L, Cepinskas G, Sandig M, Inculet R, McCormack DG, Mehta S. Albumin leak across human pulmonary microvascular vs. umbilical vein endothelial cells under septic conditions. *Microvasc Res* 2006;71:40–47.
43. Kim SJ, Eum HA, Billiar TR, Lee SM. Role of heme oxygenase 1 in TNF/TNF receptor-mediated apoptosis after hepatic ischemia/reperfusion in rats. *Shock* 2013;39:380–388.
44. Konrad FM, Knausberg U, Höne R, Ngamsri KC, Reutershan J. Tissue heme oxygenase-1 exerts anti-inflammatory effects on LPS-induced pulmonary inflammation. *Mucosal Immunol* 2016;9:98–111.
45. Wilson SJ, Keenan AK. Role of hemin in the modulation of H2O2-mediated endothelial cell injury. *Vascul Pharmacol* 2003;40:109–118.
46. Muller-Eberhard U, Javid J, Liem HH, Hanstein A, Hanna M. Plasma concentrations of hemopexin, haptoglobin and heme in patients with various hemolytic diseases. *Blood* 1968;32:811–815.
47. Wochner RD, Spilberg I, Iio A, Liem HH, Muller-Eberhard U. Hemopexin metabolism in sickle-cell disease, porphyrias and control subjects—effects of heme injection. *N Engl J Med* 1974;290:822–826.
48. Reiter CD, Wang X, Tanus-Santos JE, Hogg N, Cannon RO III, Schechter AN, Gladwin MT. Cell-free hemoglobin limits nitric oxide bioavailability in sickle-cell disease. *Nat Med* 2002;8:1383–1389.
49. Moreno-Gonzalez G, Vandenabeele P, Krysko DV. Necroptosis: a novel cell death modality and its potential relevance for critical care medicine. *Am J Respir Crit Care Med* 2016;194:415–428.